The role of subsidence in shelf widening around ocean island volcanoes: Insights from observed morphology and modeling

DOI:
10.1016/j.epsl.2018.07.007

Document Version
Accepted author manuscript

The role of subsidence in shelf widening around ocean island volcanoes: Insights from observed morphology and modeling

Rui Quartau[1,3], Alan S. Trenhaile[2], Ricardo S. Ramalho[3,4,5] and Neil C. Mitchell[6]

[1]Divisão de Geologia Marinha, Instituto Hidrográfico, Lisboa, Portugal.

[2]Department of Earth and Environmental Sciences, University of Windsor, Windsor, Canada.

[3]Instituto Dom Luiz, Faculdade de Ciências da Universidade de Lisboa, Lisboa, Portugal.

[4]School of Earth Sciences, University of Bristol, Bristol, UK.

[5]Lamont-Doherty Earth Observatory at Columbia University, New York, USA

[6]School of Earth and Environmental Sciences, University of Manchester, Manchester, UK.

Corresponding author: Rui Quartau (rui.quartau@hidrografico.pt)

Key Points: (85 characters)

- Shelf break depths on old edifices of the Azorean islands are commonly >130 m.
- Edifices have subsided significantly since their shelf breaks were formed.
- A coastal erosion model evaluates the role of subsidence in shelf widening.
- Subsidence plays a crucial role in widening and deepening insular shelves.

Abstract

On reefless volcanic islands, insular shelves are thought to have formed essentially by the combined effects of wave erosion and glacio-eustatic sea-level oscillations. Subsidence, however, has also been recognized as having an important role in the development of these morphologies. Yet, few studies have quantified the relative contribution of subsidence to shelf generation and development, particularly to shelf width. A better understanding of this contribution, however, is key to understand the long-term evolution of coasts at volcanic islands, particularly given that subsidence may exacerbate the effects of marine erosion. In this study we assess quantitatively the role of subsidence in shelf development by comparing real cross-shore shelf elevation profiles with modeled profiles using varied rates of subsidence. To achieve this, we used shelf bathymetric profiles from Faial and São Jorge islands in the Azores, which we compared with predictions of a numerical model of coastal erosion that has been calibrated previously against other field data. The first set of model runs were made to calibrate the model by determining the values that produced shelves with break depths, widths, and profile shapes that were similar to those observed. The second set of runs, which served to evaluate the contribution of subsidence to shelf widening, revealed that subsidence may have been responsible for increasing shelf widths by almost 2.5 times relative to shelves formed only by the combined effects of wave erosion and glacio-eustatic oscillations. Modeling shelf formation on the same islands but with increased subsidence rates up to 2.2 mm/year resulted in shelf profiles up to 19 km wide, a value 3 to 6 times greater than observed on these islands. Our study therefore reinforces the idea that subsidence is a key contributor to the generation of broad insular shelves, given its role in enhancing coastal retreat. Our shelf evolution modeling also suggests that, notwithstanding the crucial role subsidence plays in increasing the width of shelves, on islands subjected to energetic wave regimes (as it happens in the Azores and Hawaii), modification by erosion is important

enough to result in shelf morphologies that are not constructional in essence, but rather dominantly erosive surfaces. This study therefore contributes to a better understanding of how insular shelves and submarine terraces form and develop by proving important new quantitative insights of the role of subsidence on the generation of these morphologies.

1 Introduction

Continental and insular shelves are extremely important for our society in spite of their small size (cumulatively only cover ~8% of the total oceans by area). They are areas of terrigenous sediment input from continents and islands, where economically important mineral deposits form [Rona, 2008] and significant carbon is sequestrated [Leithold et al., 2016]. They are also the ocean area most used for navigation, recreation, fishing, aquaculture, mineral exploration and waste disposal [Chiocci and Chivas, 2014]. Hence, small environmental changes to the coastal border of these systems can have a disproportionate impact on human activities. Following the development of single-beam echo-sounders, and into the 2nd half of the 20th century, the exploration of continental shelves rapidly expanded [e.g., Dietz and Menard, 1951; Emery, 1965; Hayes, 1964; Hedberg, 1970; Inman and Nordstrom, 1971; Shepard, 1973; Vanney and Stanley, 1983]. More recently, there has been an increasing interest in improving our knowledge of the processes affecting the formation and evolution of such shelf systems [e.g., Helland-Hansen et al., 2012; O'Grady et al., 2000; Paris et al., 2016; Schlager and Adams, 2001]. The shelves of volcanic ocean islands, however, have received comparatively little attention since the seminal works of Menard [1983; 1986]. The study of insular shelves is, however, crucial to our society given that most island populations depend on the marine biological and geological resources found in these environments, as well as on the income proportioned by coastal tourism. Additionally, insular shelves and coastlines are far more exposed to rapid change than their continental counterparts, posing more serious hazards to coastal communities [Ramalho et al., 2013]. It is thus of primal importance to understand the role of different processes affecting coastal evolution and shelf development in these settings, particularly concerning marine erosion.

Volcanic oceanic islands are surrounded invariably by shelves, which are low-lying submarine zones that extend from the coast to the depth at which there is a marked increase in gradient to the submarine slopes of the volcanic edifice (Quartau et al., 2010; Ramalho et al., 2013). These shelves are thought to form mainly as wave eroded intertidal zones migrate landward and seaward with sea level changes. As a consequence, shelf width increases through time as coastlines retreat with marine erosion, leading to a common relationship between shelf age and shelf width (Menard, 1983; Le Friant et al., 2004; Llanes et al., 2009; Quartau et al., 2010). However, a closer look at the morphology of shelves reveals that they result from a more complex set of processes, including volcanism, tectonics and vertical movements, subaerial erosion, sedimentation and mass-wasting (Quartau et al., 2012; Ramalho et al., 2013). Therefore, the correlation between shelf age and shelf width is not always straightforward, especially on older islands where the combined effects of different processes can make their shelves geomorphologically more complex (Menard, 1983; Quartau et al., 2010, 2014, 2015; Romagnoli, 2013). For example, Quartau et al. (2010) used a model to investigate the role of mechanical wave erosion in the development of the shelf of Faial Island (Azores). They found that, although the shelf was mainly formed by wave erosion, other geological processes contributed to its development. The role of these processes, however, was only discussed qualitatively.

From all the mechanisms recognized as having a role in shelf development, perhaps none has fueled more discussion than subsidence. Researchers in general agree that subsidence influences shelf development (e.g., Menard, 1983; Ramalho et al., 2013; Quartau et al., 2014; Trenhaile, 2014; Ramalho et al., 2017), but its importance is still debated (e.g., Marques et al., 2016; Quartau et al., 2016). Ocean island volcanoes are generally expected to subside by varying amounts, and only very rarely are subjected to significant uplift trends (Ramalho et al., 2010a,b). Significant subsidence is expected to occur particularly during the

early shield building stages, when rapidly-growing volcanic edifices load the underlying lithosphere, causing plate flexure (Watts and ten Brink, 1989). Towards the end of the shield–building phase, when volcanoes reach their maximum size, subsidence related to flexural loading supersedes volcanic growth and volcanoes usually begin to submerge without additional topographic growth (Huppert et al., 2015). This subsidence is expected to wane rapidly (on a geological timescale) once a volcanic edifice is built, as viscous relaxation of the lithosphere gives way to its longer-term flexural strength (Brotchie and Silvester, 1969; Walcott, 1970; McNutt and Menard, 1978; Minshull et al., 2010). Islands are also generally subjected to longer-term, slower-acting subsidence on account of cooling of the underlying lithospheric plate (Stein and Stein, 1992), which may be enhanced if the lithosphere is significantly heated and 'reset' by magmatism (Detrick and Crough, 1978). The global variation of seafloor depth is generally controlled by the oceanic plates' thermal evolution, in which oceanic lithosphere cools as it spreads away from mid-ocean ridges, becoming denser as it ages, therefore resulting in a predictable bathymetric profile, with depth roughly equivalent to age$^{1/2}$ and asymptotically trending to equilibrium at ~70 Ma (Stein and Stein, 1992). Long-term island subsidence is thus dominantly controlled by thermal subsidence of the underlying plate, except when volcanic island edifices are built on stable >70 m.yr.-old lithosphere. Magmatism and hotspots swells may affect this trend by means of rejuvenating the lithosphere or more importantly by causing uplift through either the accumulation of buoyant melt residue underneath the lithosphere (Morgan et al., 1995; Ramalho et al 2010b.) or through dynamic topography (Sleep, 1990; Ribe and Christensen, 1999; Pim et al. 2008). Hotspot swell decay, however, contributes to island subsidence, at least on fast-moving plates with respect to the melting source (Morgan et al. 1995; Ramalho et al., 2013). Considerable tectonic subsidence may also affect islands that are located in diffuse extensional or

transtensional plate boundaries, as on some of the Azores Islands and in Iceland (Islam et al., 2016; Madeira et al, 2015; Marques et al., 2013).

Given these diverse mechanisms, it is not surprising that subsidence influences shelf development. However, different researchers have considered the role of subsidence in shelf development to be dominant or secondary relatively to the combined effects of marine erosion and glacio-eustatic oscillations. Marques et al. (2016), for example, suggested that subsidence takes a leading role in shelf formation, to the point that shelf morphology is essentially constructional in nature. According to this view, the shelf break corresponds to the transition between the subaerial and submarine slopes of the volcanic edifice, i.e. between subaerial and submarine lava flow sequences that have been submerged by rapid subsidence. This model might be applicable to the rare cases of island coastlines subjected to very slow marine erosion rates (e.g. the case of the younger Galapagos Islands) and/or very fast subsidence. However, its applicability to other settings has been questioned because of erosive insular shelf profiles (upwards-concave and with gradients that are significantly lower than the subaerial slopes of the volcanoes), high coastal cliffs, and possibly overestimated subsidence rates (Quartau et al., 2016). Notwithstanding these considerations, the relative role of subsidence in insular shelf development remains largely unquantified, and constitutes an important scientific question.

The purpose of this study was to quantitatively assess the role of subsidence in the formation of insular shelves. A wave erosion model was used to simulate the cross-shore shelf profiles of two subsiding islands in the Azores, to determine their rates of subsidence and to compare these profiles with those produced under otherwise similar conditions on stable landmasses. The model was used more generally, to investigate the effect of variable rates of subsidence on insular shelf formation and on the age of the shelf breaks formed under oscillating sea level conditions during the Quaternary.

2 Materials and Methods

2.1 The Azores as a case study

The Azores Archipelago is a group of relatively young volcanic islands that straddle the triple junction between the Eurasian (Eu), Nubian (Nu), and North American (NA) tectonic plates (Laughton and Whitmarsh, 1974). In the Azores, volcanism is mainly tectonically controlled and occurs along faults (fissure volcanic systems) or at fault intersections (central volcanoes), often resulting in volcanic edifices with varied ages and complex morphologies (Marques et al., 2013; Madeira et al., 2015). It is therefore not surprising that shelf width and the depth of the shelf breaks vary on different volcanic edifices, even on the same island. A rough relationship between edifice age and shelf width and depth has been established from coasts subjected to similar wave regimes (Quartau et al., 2014; Quartau et al., 2015). Crucially to this study, however, shelf breaks around the oldest sectors of some islands are significantly deeper than sea levels attained during Late Pleistocene lowstands. This suggests that subsidence played a role in shelf development on these islands (Quartau et al., 2014; 2015; 2016), which is not surprising given that the islands used in this study are located on young lithosphere and lie in the vicinities of the Terceira rift, a boundary that is mostly extensional (Madeira et al., 2015; Marques et al., 2013). The central Azores Islands are an ideal case study to quantify the contribution of subsidence to shelf development because: (1) They constitute one of the few places for which ample bathymetric data exists covering the island shelves and for which the age of the original volcanic slopes of the edifice are known; 2) The islands are subjected to both subsidence and considerable wave erosion, , allowing for an investigation of the individual role of each of these mechanisms in the generation of shelf profiles.. The Azores is therefore seen as a good representative for

122 reefless volcanic islands subjected to medium subsidence rates and subjected to energetic
123 wave regimes.

124

125 **2.2 Observed morphologies**

126 The offshore rocky edge of an insular shelf (below any sediment cover) is normally a
127 wave erosional feature, which formed when sea level was at that lowered position during a
128 lengthy period of volcanic inactivity. The two shelf areas selected for this subsidence analysis
129 (Faial and São Jorge; see Figure 1 and Table 1) lie adjacent to volcanic edifices that are the
130 oldest on each island and have shelf breaks significantly deeper than levels attained during
131 Pleistocene glacial-maxima (~130 m). Assuming these shelf breaks were cut during times of
132 low sea level, then these islands must have subsided. The lack of morphologically-preserved
133 submarine lava flows on the studied sectors of these shelves implies that no offshore volcanic
134 progradation occurred after most of the shelf was carved (Figures SM 1 and SM2 in
135 supplementary material). However, in the older sectors of these islands, there is considerable
136 variability in the depth of the shelf break due to small mass-wasting events, which caused
137 headward erosion and effective shoaling of this feature. Hence, we selected the cross-shore
138 profiles in areas least degraded by mass wasting and where deep breaks suggested maximum
139 amounts of subsidence (Figures SM 1 and SM2 in supplementary material).

140 Distinguishing erosional shelf breaks from depositional shelf breaks is complicated.
141 The outer parts of the shelves are frequently covered by sediments up to several 10s of meters
142 thick, which obscure the underlying erosional shelf surface and reduce the depth of the
143 topographic edge (Quartau et al., 2012; 2014; 2015; 2016). The thickness of the sedimentary
144 cover can only be determined with reflection seismic data, which unfortunately was not
145 available for the selected study sites. We used instead two approaches to locate the erosional

shelf edge, one more conservative that provides a shallower position (blue dashed line in Figure 2), and another less-conservative estimate that is deeper (black dashed line in Figure 2). In our more conservative approach, the erosional shelf break was inferred as being located where the tangent to the outermost shelf surface detaches from the seafloor (method 2C in Figure 2 of Wear et al., 1974). In contrast, in our less conservative approach, the break was inferred to lie where the tangent to the steepest slope gradient detaches upward from the slope profile. From previous studies of Quartau et al. (2012; 2014; 2015) using seismic reflection data, the less conservative estimate is normally closer to the true erosional shelf break, though here we consider both estimates for completeness.

2.3 The erosional model

Modeling allows the effects of changing sea level to be integrated with changes in the elevation of the land that is being eroded; hence it is particularly useful for studying the development of slowly evolving rock coasts over long periods of time. There have been several attempts to model the formation of erosional submarine shelves, although most have involved a simple rise or fall in sea level rather than the more complex changes in rates and directions that have occurred in the last few million years over multiple glacial-interglacial cycles (Trenhaile, 2000; Quartau et al., 2010; Stephenson et al., 2013). There have also been few attempts to include the additional effect of simultaneous uplift or subsidence of the land (Trenhaile, 2014).

The model that we apply here has been used previously to investigate the development of shore platforms, elevated marine terraces, and continental shelves (Trenhaile, 2000; 2014). It was also employed by Quartau et al. (2010) to simulate the formation of the submarine shelf around Faial Island in the Azores, incorporating changes in sea level during

the middle and late Quaternary. Estimates of the amount of subsidence in that paper were based on differences between the depths of shelf breaks modeled without any subsidence and the observed breaks derived from multibeam sonar and chirp and boomer seismic reflection mapping. In the present paper, which is concerned specifically with the effect of subsidence on the development of insular shelves, subsidence operated simultaneously with changes in sea level, and model runs therefore incorporated the amplifying effects of subsidence on rates of erosion due to increasing water depths and decreasing rates of wave attenuation.

In constructing the model, mechanical wave erosion was assumed to be accomplished predominantly by broken waves, from wave quarrying of rocks at or close to the water surface and abrasion in shallow-water (Trenhaile, 1987; Cruslock et al., 2010; Naylor and Stephenson, 2010). The model derivation has been described in detail previously (e.g., Trenhaile, 2000; 2002; 2014), so only a basic outline is provided here (SI units are used throughout this discussion).

According to USACE (1984), the wave stress (kg m^{-2}) at the breakers (τ_b) is given by::

$$\tau_b = 0.5\rho_w h_b \quad (1)$$

where ρ_w (1025 kg m^{-3}) is the unit weight of water and $h_b$is the breaker depth. Incorporating a surf decay function (e^{-kW_s}), which considers the width (W_s) and geologically induced surface roughness of the surf zone (k), and the minimum or threshold stress for rock erosion (τ_c), provides an expression for the excess surf stress at the shoreline (τ_e):

$$\tau_e = 0.5\rho_w h_b e^{-kW_s} - \tau_c \quad (2)$$

Waves break when:

192 $$h_b = 1.28H_b \quad (3)$$

193 where H_b is the breaker wave height, calculated from the wave period and deep-water wave
194 height using Komar and Gaughan's (1972) equation. Therefore:

195 $$\tau_e = 656H_b e^{-kW_s} - \tau_c \quad (4)$$

196 To determine the annual amount of erosion (E_{WL}) at each intertidal elevation, the
197 contribution of each type of wave was summed, according to its frequency (W_n, the number
198 of waves of each type per hour) and the tidal duration (T_d, the annual number of hours that
199 the tide occupies each intertidal elevation). For example, at the mean high water spring
200 ($MHWS$) tidal level the annual amount of erosion (m) was equal to:

201 $$E_{MHWS} = MT_d W_n 656H_b e^{-kW_s} - \tau_c \quad (5)$$

202 Where the scaling coefficient M ($6.5 \times 10^{-10}\ m^3\ kg^{-1}$) converts excess surf stress
203 into erosional units. Calculations were made at five, equally-spaced elevations (0.4 m apart)
204 within the intertidal zone, at the $MHWS$, mean high water neap, mid-tide (MT), mean low
205 water neap ($MLWN$), and mean low water spring tidal levels.

206 A decay function was also used to represent slower rates of erosion (E_u) accomplished by
207 wave-generated bottom currents and abrasion below the sea surface:

208 $$E_u = E_y e^{sh} \quad (6)$$

209 Where E_y is the annual erosion at the waterline, with subscript y referring to each
210 intertidal level or subtidal interval (0.4 m apart) at higher elevations, s is a depth decay
211 constant ($s = 1\ \mathrm{m}^{-1}$ in the model runs) and h is the local water depth (m). This equation was
212 used to calculate the annual amount of submarine erosion when the waterline was at each of

213 the five intertidal elevations, from the *MHWN* tidal level to half the wavelength of the wave
214 below the *MLWS* tidal level. The submarine erosional contribution (equation 6) was then
215 combined with the erosion occurring at the water surface (equation 5) to determine the total
216 annual erosion at each intertidal and subtidal elevation (Figure 3). These totals were then
217 multiplied by 25 to represent the erosion occurring over 25-year iteration intervals.

218 Model parameters, including M, s, τ_c, and k, were determined by Trenhaile
219 (2000), who used model equations for the surf stress at the shoreline, and for erosion rates at
220 the shoreline and in the submarine domain to obtain a range of values that encompassed the
221 wide variety of conditions existing in the field. The same tidal and wave conditions were used
222 as in the previous study of Faial Island (Quartau et al., 2010), using Carvalho's (2003)
223 hindcast data to determine the percentage frequency of nine waves with different significant
224 wave heights (ranging from 1- 16 m) and periods according to the orientation (in 45^o units) of
225 each coastal sector. Wave conditions for each of the two study areas were represented by the
226 combined data from directions normal to the coast and from directions ±45° to the normal.
227 For example, the essentially northerly-oriented Faial coastal sector was represented by a
228 combination of the wave data from the northwest, north, and the northeast. The lack of
229 relevant data prevented the effect of shelter and reduced wave fetches from the southwest on
230 São Jorge Island and from the northeast on Faial Island being considered in this study. Tidal
231 duration values were calculated for Porto da Horta on Faial Island using Smart and Hale's
232 (1987) program and tidal data from Instituto Hidrográfico (2007). Bintanja and van de Wal's
233 (2008) composite sea-level curve (Figure 4), which used a simple ocean-temperature model
234 to correct benthic $\delta^{18}O$ records from 57 globally distributed sediment cores, was used for
235 periods corresponding to the estimated volcanic age of each coastal sector, which was 1.3 Ma
236 on São Jorge and 0.85 Ma on Faial (Figures SM1 and SM2). In most model runs, the initial
237 linear surface had a 25° gradient corresponding roughly to the degraded slopes of the

238 volcanic hinterlands found in each of the two sites and with the gradients of the uneroded
239 slopes preserved beneath the shelf breaks. Otherwise identical runs with initial slope
240 gradients of 5º–30º demonstrated, as previously shown by Quartau et al. (2010), that the
241 gradient of the initial slope had little effect on the gradient of the simulated shelf profiles,
242 given the fairly rapid erosion and the relatively long timescale considered in the simulations.
243 We did not include an isostatic term to account the response of the shelf to erosion because
244 we believe it would be negligible. Smith & Wessel (2000) modeled the isostatic effect of the
245 giant landslides of Hawaii, a much larger volume and the smaller slides (e.g., Alika I and II,
246 with volumes of one order magnitude greater than our modeled shelf erosion) produced only
247 17 m and 7 m uplift for T_e corresponding to 25 and 40 km, respectively.

248 There were three types of model run. The first was designed to replicate the shelves in
249 the two study areas, using the relevant orientation-dependent wave conditions for the two
250 profile sites. Runs were carried out in each study area for which we have estimated maximum
251 and minimum amounts of subsidence (respectively red and green dots in Figure 5). These
252 runs used a variety of k values (surface roughness - surf attenuation rates which control shelf
253 width) and subsidence rates (which determine the depth of the shelf break) to determine the
254 values that produced shelves with break depths, widths, and profile shapes that were similar
255 to those observed. These optimum values were then used in a second series of runs that
256 employed the same glacial-interglacial changes in sea level but with no changes in the
257 elevation of the land. The third type of run, using the values for *k* that best simulated the four
258 shelves, were made to investigate further the effect of subsidence on shelf morphology. These
259 runs were made only for the deeper shelf break estimates of Faial and São Jorge with
260 subsidence ranging from less than 50 m to almost 2000 m, attained during the time elapsed
261 since the original volcanic slopes were formed.

262

4 Results

The modeling results are shown in Figure 5 and Table 1. The model recorded the lowest level of erosion and when it occurred (as labeled on the profiles in Figure 5). Linear subsidence was chosen for the sake of simplicity, although we are aware that subsidence of ocean islands typically operates rapidly during the initial stages of island building, and wanes to a slow trend after that (Sharp & Renne, 2005; Watts & Zhong, 2000). Rates of subsidence were calculated from the following expression assuming subsidence has been constant (as opposed to being episodic or accelerating or retarding).

$$(A\text{-}R) / T \qquad (5)$$

Where A is the original, formative, elevation of the shelf break before subsidence, R is our estimate of the present shelf break depth and T is the time elapsed since the shelf break was cut as calculated by the model during each run. The amount and rate of subsidence (Table 1) is therefore based on the age of the edge as well as its depth.

According to our modelling, subsidence increased the width of the shelf by 2.00 to 3.42 times, when compared with scenarios without subsidence (Figure 5 and Table 1). Modeling with hypothetical higher subsidence scenarios (Figure 6 and Table 2) suggests that there is a linear relationship between subsidence (or subsidence rates) and shelf width for both islands. The curve for São Jorge Island is steeper because the island is older and wave erosion has been acting for a longer period. Table 2 also shows that for islands with such ages, exposed to similar coastal erosion rates and wave properties, when subjected to subsidence rates over 0.11 mm/yr (São Jorge) or 0.17 mm/yr (Faial), the contribution of subsidence to shelf widening surpasses that of wave erosion, i.e, subsidence leads to more

than a twofold increase in shelf width. Notwithstanding this observation, the modeling shows that shelf profiles on these islands are unequivocally erosional in nature and not constructional as suggested by Marques et al. (2016). In addition, morphological evidence (Figure 5 and figures SM 1 and SM2 in supplementary material) attests that these shelves are old and subjected to continuous coastal recession, because: (1) shelf erosional profiles are sharply angular, with high cliffs and submarine slopes that extend below the shelf edge; and, (2) there are no morphologically-preserved submarine lava flows on the these areas of the shelves that would imply recent volcanic progradation.

5 How does subsidence help to widen shelves?

There are two main reasons why rising relative sea level promotes the widening of erosion surfaces. First, it increases nearshore water depths and lowers rates of wave attenuation, causing the breaker zone to migrate closer to shore. This reduces the energy lost by waves in crossing turbulent surf zones and increases the amount of energy expended at the cliff foot (Trenhaile, 2014). The effect of rising relative sea level would have been particularly pronounced following the end of each glacial period, especially on subsiding landmasses. Second, rising relative sea level amplifies the range of elevations, extending from essentially the present sea level to the shelf break, over which waves have operated. The effect of this factor is therefore closely related to the depth of the shelf break.

The shelf break marks the depth below which marine erosional processes have been ineffective. On stable landmasses, this corresponds to the elevation of the low tidal level (or, depending on submarine erosional efficacy, the shallow subtidal zone) of the lowest, glacial sea level. Conversely, on subsiding coasts, the model demonstrated that the age and depth of shelf breaks are determined by the elevation of the formative sea-levels and the time and rate

311 that the land has been subsiding since the edges were cut. For instance, a slope cut during an
312 early -50 m low sea level would form a break, which followed by 60 m of subsidence, would
313 end up in a position lower than what erosion would be able to accomplish during a much later
314 -100 m sea-level stand. This is the case for the two coasts that were modeled (see time labels
315 in Figure 5).

316 On subsiding landmasses, the depth of the shelf break (Sb) is related to:

317 $$Sb = LT_e + (Sr \times T) \quad (6)$$

318 Where LT_e is the elevation of the low tidal level or shallow subtidal zone during the
319 period of formation, Sr is the annual amount of landmass subsidence, and T is the elapsed
320 time since formation of the shelf break. The shelf break corresponds to the glacial sea level
321 that produced the highest Sb value, and was therefore below, and protected, from
322 modification in the intertidal zones of later glacial sea levels because of either rapid
323 subsidence or shallower lowstands or the combination of these two. With shelf gradients
324 related to the same variables as modern intertidal shore platforms, including tidal range and
325 rock resistance (Trenhaile, 1987; Pérez-Alberti et al., 2012; Matsumoto et al., 2017), the
326 greater the subsidence of a landmass the deeper the shelf break, and consequently, the wider
327 the shelf (Table 2).

328 The model also suggested that on rapidly subsiding landmasses, the age (time of
329 formation) of the shelf break tends to correspond to glacial periods preceding the middle
330 Quaternary Transition (MQT), about 0.8 Myr ago (Figure 4). Although these glacial sea
331 levels were not as low as those occurring after the MQT, rapid subsidence was able to carry
332 them to depths below the level of subsequent wave action. Conversely, on slowly subsiding
333 land masses the shelf break is more likely to have formed in the early Middle Quaternary
334 when the amplitude of the sea level oscillations roughly doubled, with glacial sea levels that

reached below the elevation of older, although slightly subsided, pre-MQT shelf breaks (Table 2).

6 Implications of this study

The model results suggest that subsidence can exert a strong influence on the width of submarine terraces and shelves. This can be inferred from the trends towards greater subsidence in Figure 6 and Table 2; islands with faster subsidence have significantly wider shelves or submarine terraces than islands with slower subsidence. This effect is not only because the increase of the submarine area but also because erosion is faster on islands with high subsidence rates. For example, there are wide submarine terraces on the rapidly subsiding Hawaiian islands, where the deepest shelf breaks are at depths of a little below -1800m (e.g., the SE border of the Hana Ridge, which is about 70 km from the present coast) (Faichney et al., 2010). Hawaiian subsidence rates can be one order of magnitude greater (average ~2 mm/yr according to Table 1 of Huppert et al., 2015) than those in the Azores (Table 1), and the width of the Hawaiian terraces is much greater (e.g., maximum shelf width of 5 km for São Jorge Island). These differences can be attributed in part to different subsidence rates, with model simulations (Table 2) suggesting that insular shelves up to 19 km in width could have developed in the Azores if subsidence rates had been similar to those of the Hawaiian Islands. The Azores shelves are clearly narrower than this and the islands themselves are smaller (Faial and São Jorge, are respectively 1043 m and 1053 m in elevation and 14 to 12 km in width), which means they would have been drowned by the combined effects of subsidence and erosion if subjected to such high subsidence rates. The greater width of Hawaiian shelves might also be attributed in part to rapid subsidence coupled with shallow shields that lead to marine erosion acting on only superficial lava flows. Conversely,

slower subsidence and steeper subaerial volcanoes in the Azores might have resulted in slower erosion of more deeply buried and hence compacted/cemented lavas.

It has been frequently argued that, in Hawai'i, the edge of submarine terraces results from constructional processes (lava entering the water, creating a slope break and submergence due to rapid subsidence) (Moore and Clague, 1992). However, as we have seen in the Azores, a setting with similar wave conditions (Stopa et al., 2011; Rusu and Guedes Soares, 2012), shelf profiles are erosional rather than constructional, even if the islands were subjected to extreme subsidence rates (Table 2). Thus, our study indicates that some of the submarine terraces on the Hawaiian Archipelago might also be erosional in nature, notwithstanding that coral reef growth and subsidence had a greater influence than wave erosion in terrace formation. We therefore postulate that, unless subjected to very extreme subsidence rates and very low erosional rates, or subjected to the combined effects of fast coral accretion, subsidence, and low erosion rates, volcanic insular shelves are dominantly erosive in nature and rarely preserve the original constructional slope profile.

7 Conclusions

Understanding how insular shelves form and develop is crucial to our comprehension of the long-term evolution of the coastal zones of volcanic islands, with implications that can, on occasions, be extrapolated to shorter timescales. Here, we have explored the long-term contribution of subsidence in facilitating and enhancing marine erosion and consequently shoreline retreat on volcanic oceanic islands.

The combination of observed morphology with numerical wave erosion modeling suggests that subsidence significantly affects shelf development, in particular shelf width. Thus, rates of shelf widening are not only a function of wave energy, time of exposure, and

383 glacio-eustatic oscillations. Islands that have suffered greater net subsidence tend to develop
384 wider shelves as opposed to those that have suffered little or no subsidence. In the case of the
385 studied islands, and for subsidence rates >0.11 mm yr^{-1} (São Jorge) or >0.17 mm yr^{-1} (Faial),
386 the contribution of subsidence to shelf widening surpasses the role of wave erosion.
387 Effectively, the higher the subsidence rate, the greater is its contribution to final shelf or
388 terrace width, as supported by widespread evidence in the Azores Archipelago and likely also
389 in other island settings such as Hawai'i. Nevertheless, our simulated profiles also show that
390 erosion is important enough to result in shelf morphologies that are not constructional in
391 essence, i.e., subsidence assists wave erosion by exposing a greater portion of a volcano to
392 erosional modification. These results therefore provide important new quantitative constrains
393 on the mechanisms that generate insular shelves and submarine terraces, contributing to our
394 stepwise scientific understanding of their morphology and evolution.

395

396 **Acknowledgments**

397 Rui Quartau and Ricardo Ramalho acknowledge their IF/00635/2015 and IF/01641/2015
398 research contracts funded by Fundação para a Ciência e a Tecnologia. We thank Marques et
399 al. (2016) for kick starting the discussion on the role of subsidence in the evolution of
400 volcanic islands. We also acknowledge two anonymous reviewers and the Editor Tamsin
401 Mather for constructive suggestions that helped improving this manuscript.

402

403 **References**

404 Bintanja, R., van de Wal, R.S.W., 2008. North American ice-sheet dynamics and the onset of
405 100,000-year glacial cycles. Nature 454, 869-872.

406 Brotchie, J.F., Silvester, R., 1969. On crustal flexure. J. Geophys. Res. 74, 5240-5252.

407 Carvalho, F., 2003. Elementos do clima de agitação marítima no grupo central dos Açores.
408 Instituto de Meteorologia, Lisboa, p. 97.

409 Chiocci, F.L., Chivas, A.R., 2014. An overview of the continental shelves of the world, in:
410 Chiocci, F.L., Chivas, A.R. (Eds.), Continental Shelves of the World.: Their Evolution
411 During the Last Glacio-Eustatic Cycle. Geological Society, London, Memoirs, 41, pp. 1-5.

412 Cruslock, E.M., Naylor, L.A., Foote, Y.L., Swantesson, J.O.H., 2010. Geomorphologic
413 equifinality: A comparison between shore platforms in Höga Kusten and Fårö, Sweden and
414 the Vale of Glamorgan, South Wales, UK. Geomorphology 114, 78-88.

415 Detrick, R.S., Crough, S.T., 1978. Island subsidence, hot spots, and lithospheric thinning.
416 Journal of Geophysical Research: Solid Earth 83, 1236-1244.

417 Dietz, R.B., Menard, H.W., 1951. Origin of abrupt change in slope at continental shelf
418 margin Am. Assoc. Petrol. Geol. Bull. 35, 1994-2016.

419 Emery, K.O., 1965. Characteristics of continental shelves and slopes. Am. Assoc. Petrol.
420 Geol. Bull. 49, 1379-1384.

421 Faichney, I.D.E., Webster, J.M., Clague, D.A., Paduan, J.B., Fullagar, P.D., 2010. Unraveling
422 the tilting history of the submerged reefs surrounding Oahu and the Maui-Nui Complex,
423 Hawaii. Geochem. Geophys. Geosyst. 11, Q07002.

424 Hayes, M.O., 1964. Lognormal distribution of inner continental shelf widths and slopes.
425 Deep Sea Research and Oceanographic Abstracts 11, 53-78.

Hedberg, H.D., 1970. Continental margins from viewpoint of the petroleum geologist. Am. Assoc. Petrol. Geol. Bull. 54, 3-43.

Helland-Hansen, W., Steel, R.J., Somme, T.O., 2012. Shelf genesis revisited. J. Sediment. Res. 82, 133-148.

Hildenbrand, A., Madureira, P., Marques, F.O., Cruz, I., Henry, B., Silva, P., 2008. Multi-stage evolution of a sub-aerial volcanic ridge over the last 1.3 Myr: S. Jorge Island, Azores Triple Junction. Earth Planet. Sci. Lett. 273, 289-298.

Hildenbrand, A., Marques, F.O., Costa, A.C.G., Sibrant, A.L.R., Silva, P.F., Henry, B., Miranda, J.M., Madureira, P., 2012. Reconstructing the architectural evolution of volcanic islands from combined K/Ar, morphologic, tectonic, and magnetic data: The Faial Island example (Azores). J. Volcanol. Geotherm. Res. 241-242, 39-48.

Huppert, K.L., Royden, L.H., Perron, J.T., 2015. Dominant influence of volcanic loading on vertical motions of the Hawaiian Islands. Earth Planet. Sci. Lett. 418, 149-171.

Inman, D., Nordstrom, K., 1971. On the tectonic and morphologic classification of coasts. J. Geol. 79, 1-21.

Instituto Hidrográfico, 2007. Tabela de marés do Arquipélago dos Açores. Instituto Hidrográfico, Lisboa.

Islam, M.T., Sturkell, E., LaFemina, P., Geirsson, H., Sigmundsson, F., Olafsson, H., 2016. Continuous subsidence in the Thingvellir rift graben, Iceland: Geodetic observations since 1967 compared to rheological models of plate spreading. J. Geophys. Res. -Solid Earth 121, 321-338.

Komar, P.D., Gaughan, M.K., 1972. Airy Wave Theory and Breaker Height Prediction, in: American Society of Civil Engineers (Ed.), 13th Coastal Engineering Conference, Reston, pp. 405-418.

Laughton, A.S., Whitmarsh, R.B., 1974. The Azores-Gibraltar Plate Boundary, in: Kristjansson, L. (Ed.), Geodynamics of Iceland and the North Atlantic Area. Springer Netherlands, pp. 63-81.

Le Friant, A., Harford, C.L., Deplus, C., Boudon, G., Sparks, R.J.S., Herd, R.A., Komorowski, J.-C., 2004. Geomorphological evolution of Monserrat (West Indies): importance of flank collapse and erosional processes. J. Geol. Soc. London 161, 147-160.

Leithold, E.L., Blair, N.E., Wegmann, K.W., 2016. Source-to-sink sedimentary systems and global carbon burial: A river runs through it. Earth-Sci. Rev. 153, 30-42.

Llanes, P., Herrera, R., Gómez, M., Muñoz, A., Acosta, J., Uchupi, E., Smith, D., 2009. Geological evolution of the volcanic island La Gomera, Canary Islands, from analysis of its geomorphology. Mar. Geol. 264, 123-139.

Madeira, J., Brum da Silveira, A., Hipólito, A., Carmo, R., 2015. Active tectonics in the central and eastern Azores islands along the Eurasia–Nubia boundary: a review, in: Gaspar, J.L., Guest, J.E., Duncan, A.M., Barriga, F.J.A.S., Chester, D.K. (Eds.), Geological Society, London, Memoirs, 44, pp. 15-32.

Marques, F.O., Catalão, J.C., DeMets, C., Costa, A.C.G., Hildenbrand, A., 2013. GPS and tectonic evidence for a diffuse plate boundary at the Azores Triple Junction. Earth Planet. Sci. Lett. 381, 177-187.

Marques, F.O., Hildenbrand, A., Zanon, V., Boulesteix, T., 2016. Comment on "The insular shelves of the Faial–Pico Ridge (Azores archipelago): a morphological record of its evolution" by Quartau et al. (2015), doi:10.1002/2015GC005733. Geochem, Geophys, Geosyst.

Matsumoto, H., Dickson, M.E., Masselink, G., 2017. Systematic analysis of rocky shore platform morphology at large spatial scale using LiDAR-derived digital elevation models. Geomorphology 286, 45-57.

McNutt, M., Menard, H.W., 1978. Lithospheric flexure and uplifted atolls. J. Geophys. Res.: Solid Earth 83, 1206-1212.

Menard, H.W., 1983. Insular erosion, isostasy, and subsidence. Science 220, 913-918.

Menard, H.W., 1986. Islands. Scientific American Books, New York.

Minshull, T.A., Ishizuka, O., Garcia-Castellanos, D., 2010. Long-term growth and subsidence of Ascension Island: Constraints on the rheology of young oceanic lithosphere. Geophys. Res. Lett. 37, n/a-n/a.

Mitchell, N.C., Beier, C., Rosin, P., Quartau, R., Tempera, F., 2008. Lava penetrating water: submarine lava flows around the coasts of Pico Island, Azores. Geochem. Geophys. Geosyst. 9, Q03024.

Moore, J.G., Clague, D.A., 1992. Volcano growth and evolution of the island of Hawaii. Geol. Soc. Am. Bull. 104, 1471-1484.

Morgan, J. P., Morgan, W. J. & Price, E, 1995. Hotspot melting generates both hotspot volcanism and a hotspot swell? J. Geophys. Res. 100, 8045–8062.

Naylor, L.A., Stephenson, W.J., 2010. On the role of discontinuities in mediating shore platform erosion. Geomorphology 114, 89-100.

O'Grady, D.B., Syvitski, J.P.M., Pratson, L.F., Sarg, J.F., 2000. Categorizing the morphologic variability of siliciclastic passive continental margins. Geology 28, 201-210.

Paris, P.J., Walsh, J.P., Corbett, D.R., 2016. Where the continent ends. Geophys. Res. Lett. 43, 2016GL071130.

Pérez-Alberti, A., Trenhaile, A.S., Pires, A., López-Bedoya, J., Chaminé, H.I., Gomes, A., 2012. The effect of boulders on shore platform development and morphology in Galicia, north west Spain. Cont. Shelf Res. 48, 122-137.

Pim, J., Watts, A. B., Grevemeyer, I. & Krabbenhoeft, A., 2008. Crustal structure and origin of the Cape Verde Rise. Earth Planet. Sci. Lett. 272, 422–428.

Quartau, R., Hipólito, A., Romagnoli, C., Casalbore, D., Madeira, J., Tempera, F., Roque, C., Chiocci, F.L., 2014. The morphology of insular shelves as a key for understanding the geological evolution of volcanic islands: Insights from Terceira Island (Azores). Geochem. Geophys. Geosyst. 15, 1801–1826.

Quartau, R., Madeira, J., Mitchell, N.C., Tempera, F., Silva, P.F., Brandão, F., 2015. The insular shelves of the Faial-Pico Ridge: a morphological record of its geologic evolution (Azores archipelago). Geochem. Geophys. Geosyst. 16, 1401–1420.

Quartau, R., Madeira, J., Mitchell, N.C., Tempera, F., Silva, P.F., Brandão, F., 2016. Reply to comment by Marques et al. on "The insular shelves of the Faial-Pico Ridge (Azores archipelago): A morphological record of its evolution". Geochem. Geophys. Geosyst. 17, 633-641.

Quartau, R., Mitchell, N.C., 2013. Comment on "Reconstructing the architectural evolution of volcanic islands from combined K/Ar, morphologic, tectonic, and magnetic data: The Faial Island example (Azores)" by Hildenbrand et al. (2012) [J. Volcanol. Geotherm. Res. 241-242 (2012) 39-48]. J. Volcanol. Geotherm. Res. 255, 124-126.

Quartau, R., Tempera, F., Mitchell, N.C., Pinheiro, L.M., Duarte, H., Brito, P.O., Bates, R., Monteiro, J.H., 2012. Morphology of the Faial Island shelf (Azores): The interplay between volcanic, erosional, depositional, tectonic and mass-wasting processes. Geochem. Geophys. Geosyst., 13, Q04012, doi:10.1029/2011GC003987.

Quartau, R., Trenhaile, A.S., Mitchell, N.C., Tempera, F., 2010. Development of volcanic insular shelves: Insights from observations and modelling of Faial Island in the Azores Archipelago. Mar. Geol. 275, 66-83.

Ramalho, R.S., Helffrich, G., Madeira, J., Cosca, M., Thomas, C., Quartau, R., Hipólito, A., Rovere, A., Hearty, P.J., Ávila, S.P., 2017. Emergence and evolution of Santa Maria Island (Azores)—The conundrum of uplifted islands revisited. Geol. Soc. Am. Bull. 129, 372-390.

Ramalho, R.S., Helffrich, G., Schmidt, D.N., Vance, D., 2010a. Tracers of uplift and subsidence in the Cape Verde archipelago. J. Geol. Soc. London 167, 519-538.

Ramalho, R., Helffrich, G., Cosca, M., Vance, D., Hoffmann, D. and Schmidt, D.N., 2010b. Episodic swell growth inferred from variable uplift of the Cape Verde hotspot islands. Nat. Geosci. 3, 774–777.

Ramalho, R.S., Quartau, R., Trenhaile, A.S., Mitchell, N.C., Woodroffe, C.D., Ávila, S.P., 2013. Coastal evolution on volcanic oceanic islands: A complex interplay between volcanism, erosion, sedimentation, sea-level change and biogenic production. Earth-Sci. Rev. 127, 140-170.

Ribe, N. M. and Christensen, U. R., 1999. The dynamical origin of Hawaiian volcanism. Earth Planet. Sci. Lett. 171, 517–531.

Romagnoli, C., 2013. Characteristics and morphological evolution of the Aeolian volcanoes from the study of submarine portions, in: Lucchi, F., Peccerillo, A., Keller, J., Tranne, C.A., Rossi, P.L. (Eds.), Geological Society, London, Memoirs, 37, pp. 13-26.

Rona, P.A., 2008. The changing vision of marine minerals. Ore Geol. Rev. 33, 618-666.

Rusu, L., Guedes Soares, C., 2012. Wave energy assessments in the Azores islands. Renew. Energy 45, 183-196.

Schlager, W., Adams, E.W., 2001. Model for the sigmoidal curvature of submarine slopes. Geology 29, 883-886.

Sharp, W.D., Renne, P.R., 2005. The 40Ar/39Ar dating of core recovered by the Hawaii Scientific Drilling Project (phase 2), Hilo, Hawaii. Geochem. Geophys. Geosyst. 6, Q04G17, doi:10.1029/2004GC000846.

547 Shepard, F.P., 1973. Submarine Geology, 3rd Edition. Harper & Row, New York.Sleep, N.
548 H., 1990. Hotspots and mantle plumes: Some phenomenology. J. Geophys. Res. 95, 6715–
549 6736.

550 Smart, C.C., Hale, P.B., 1987. Exposure and inundation statistics from published tide tables.
551 Comput. Geosci. 13, 357-368.

552 Smith, J.R., Wessel, P., 2000. Isostatic Consequences of Giant Landslides on the Hawaiian
553 Ridge. Pure Appl. Geophys. 157, 1097-1114.

554 Stein, C.A., Stein, S., 1992. A model for the global variation in oceanic depth and heat flow
555 with lithospheric age. Nature 359, 123-129.

556 Stephenson, W.J., Dickson, M.E., Trenhaile, A.S., 2013. Rock Coasts, in: Shroder, J.F. (Ed.),
557 Treatise on Geomorphology. Academic Press, San Diego, pp. 289-307.

558 Stopa, J.E., Cheung, K.F., Chen, Y.-L., 2011. Assessment of wave energy resources in
559 Hawaii. Renewable Energy 36, 554-567.

560 Trenhaile, A.S., 1987. The geomorphology of rock coasts. Oxford University Press, Oxford.

561 Trenhaile, A.S., 2000. Modeling the development of wave-cut platforms. Mar. Geol. 166,
562 163-178.

563 Trenhaile, A.S., 2014. Modelling the effect of Pliocene–Quaternary changes in sea level on
564 stable and tectonically active land masses. Earth Surf. Proc. Land. 39, 1221-1235.

565 USACE., 1984. Shore Protection Manual (4th edition). U.S. Army Corps of Engineers:
566 Washington, D.C.

567 Vanney, J.-R., Stanley, D.J., 1983. Shelfbreak physiography: an overview, in: Stanley, D.J.,
568 Moore, G.T. (Eds.), The shelfbreak: Critical interface on Continental Margins. Society of
569 Economic Paleontologists and Mineralogists, Tulsa, Oklahoma, pp. 1-24.

570 Walcott, R.I., 1970. Flexural rigidity, thickness, and viscosity of the lithosphere. J. Geophys.
571 Res. 75, 3941-3954.

572 Watts, A.B., Zhong, S., 2000. Observations of flexure and the rheology of oceanic
573 lithosphere. Geophys. J. Int. 142, 855-875.

574 Wear, C.M., Stanley, D.J., Boula, J.E., 1974. Shelfbreak physiography between Wilmington
575 and Norfolk canyons. Mar. Technol. Soc. J. 8(4), 37-48.
576

577 **Figure 1**. Elevation and bathymetric map of the islands of Faial and São Jorge in the Azores
578 Archipelago. Bathymetry is a compilation of data from *Mitchell et al.* (2008), *Quartau et al.*
579 (2015; 2016), and the EMODNET web portal (http://portal.emodnet-bathymetry.eu). Digital
580 topography was derived from Instituto Geográfico do Exército 1:25 000 maps. Irregular black
581 lines locate the shelf edges. Dashed blue curves locate the shelf edges surrounding the oldest
582 volcanic edifices of Faial (Quartau and Mitchell, 2013) and São Jorge Islands (Quartau et al.,
583 2016). Black straight lines locate the topographic profiles of Figures 2, where no significant
584 erosion by mass wasting exists.

585

586 **Figure 2**. Cross-shore topographic profiles located on Figure 1 (3:1 vertical exaggeration).
587 Brown lines represent the subaerial and seafloor surfaces. The blue and black solid lines
588 represent tangents to the outermost shelf surface and to the uppermost slope with the highest
589 gradient. These were used to locate the shallow and deeper erosional shelf break estimates
590 (respectively green and red dots; Table 1). Dashed black and blue lines represent
591 respectively, the cross-shore erosional shelf below the sedimentary cover, for the deeper and
592 the shallower shelf break estimates.

593

594 **Figure 3**. Graphical representation of intertidal (E plus tidal subscript) and subtidal (Eu)
595 erosional increments in the model. The tidal acronyms MHWS, MHWN, MT, MLWN and
596 MLWS refer to the mean high water spring, mean high water neap, mid-tide, mean low water
597 neap and mean low water spring levels, respectively. Td, followed by a tidal subscript, refers
598 to the tidal duration value at the corresponding tidal level. The MHWS level has no subtidal
599 erosion but the erosion at all other intertidal levels was the sum of the erosion accomplished

600 by each of the five types of wave operating at that elevation, and the subtidal erosion that
601 occurs when the water surface is at a higher elevation.

602

603 **Figure 4**. Changes in sea level over the last 1.3 m.yr, showing the increase in oscillation
604 amplitude and decrease in frequency after the Mid-Quaternary Transition (MQT), about 0.8
605 m.yr ago (Bintanja and van de Wal, 2008).
606

607 **Figure 5**. Simulated cross-shore shelf profiles, with subsidence (dark blue) and without
608 subsidence (light blue). Brown solid lines represent the present-day cross-shore profiles.
609 Dashed black lines represent the cross-shore erosional shelf below the sedimentary cover.
610 Numbers next to profiles (e.g. 630100 BP) represent the time elapsed in years since the shelf
611 break was last cut in the model.

612

613 **Figure 6**. Relation between landmass subsidence and shelf widening due to the increasing
614 erosional effect caused by subsidence. Blue and black dots represent respectively estimates
615 for Faial and São Jorge Islands.

616

617 **Table 1.** Ages of the oldest volcanic edifices at Faial and São Jorge Islands (Figures 1, SM1
618 and SM2), their erosional shelf break depths estimated as in Figure 2; subsidence rates
619 estimated by the modeling, and contribution of subsidence to increase the shelf width on
620 subsiding shelves due to the combined effect of subsidence and increase in cliff erosion.
621

	Age of volcanism (Myr)	Erosional shelf break depth (m)		Model subsidence (mm/yr)		Contribution of subsidence to shelf width increase (%)	
		Min	Max	Min	Max	Min	Max
Faial	0.85[1]	171	280	0.07	0.22	100	127
São Jorge	1.32[2]	262	426	0.14	0.28	124	242

622 [1]From Hildenbrand et al. (2012)

623 [2]From Hildenbrand et al. (2008)

624

625 **Table 2.** Results of the modeling of increasing subsidence values and its impact shelf
626 widening of the Faial and São Jorge sectors studied.

627

Subsidence (m)		Subsidence rate (mm/yr)		Shelf width (m)		Contribution of subsidence to shelf width increase (%)		Age of shelf break (yr)	
Faial	São Jorge	Faial	São Jorge	Faial	São Jorge	Faial	São Jorge	Faial	São Jorge
0.00	0.00	0.00	0.00	1405.00	1547.00	0.00	0.00	630100	630100
47.22	44.00	0.06	0.03	1808.30	1857.96	28.70	20.10	630100	630100
60.71	66.00	0.07	0.05	1935.90	2098.00	37.79	35.62	630100	630100
85.00	110.00	0.10	0.08	2165.80	2591.50	54.15	67.52	630100	1250050
106.25	146.50	0.13	0.11	2354.10	3012.70	67.55	94.74	630100	1250050
141.67	188.50	0.17	0.14	2682.40	3493.50	90.92	125.82	800075	1250050
170.00	235.50	0.20	0.18	2951.40	4004.90	110.06	158.88	800075	1250050
188.50	286.50	0.22	0.22	3112.40	4535.10	121.52	193.15	800075	1250050
212.50	347.00	0.25	0.26	3317.80	5139.20	136.14	232.20	800075	1250050
265.63	366.50	0.31	0.28	3750.60	5331.00	166.95	244.60	800075	1250050
326.92	388.00	0.38	0.29	4244.30	5537.30	202.09	257.94	800075	1290125
425.00	412.50	0.50	0.31	5040.00	5777.20	258.72	273.45	800075	1290125
531.20	507.50	0.62	0.38	5849.20	6699.90	316.31	333.09	800075	1290125
708.30	660.00	0.83	0.50	7138.00	8149.20	408.04	426.77	800225	1290125
1062.50	825.00	1.25	0.63	9799.00	9654.30	597.44	524.07	800075	1290425
1416.67	942.50	1.67	0.71	12740.80	10675.60	806.82	590.08	835600	1290125
1545.45	1100.00	1.82	0.83	13764.60	12070.70	879.69	680.27	849925	1290125
1700.00	1320.00	2.00	1.00	15105.30	14039.80	975.11	807.55	849925	1290125

	1888.50	1650.00	2.22	1.25	16805.00	16956.50	1096.09	996.09	849925	1320000
		1885.50		1.43		19131.50		1136.68		1320000

628

629

Figure 1

Click here to download high resolution image

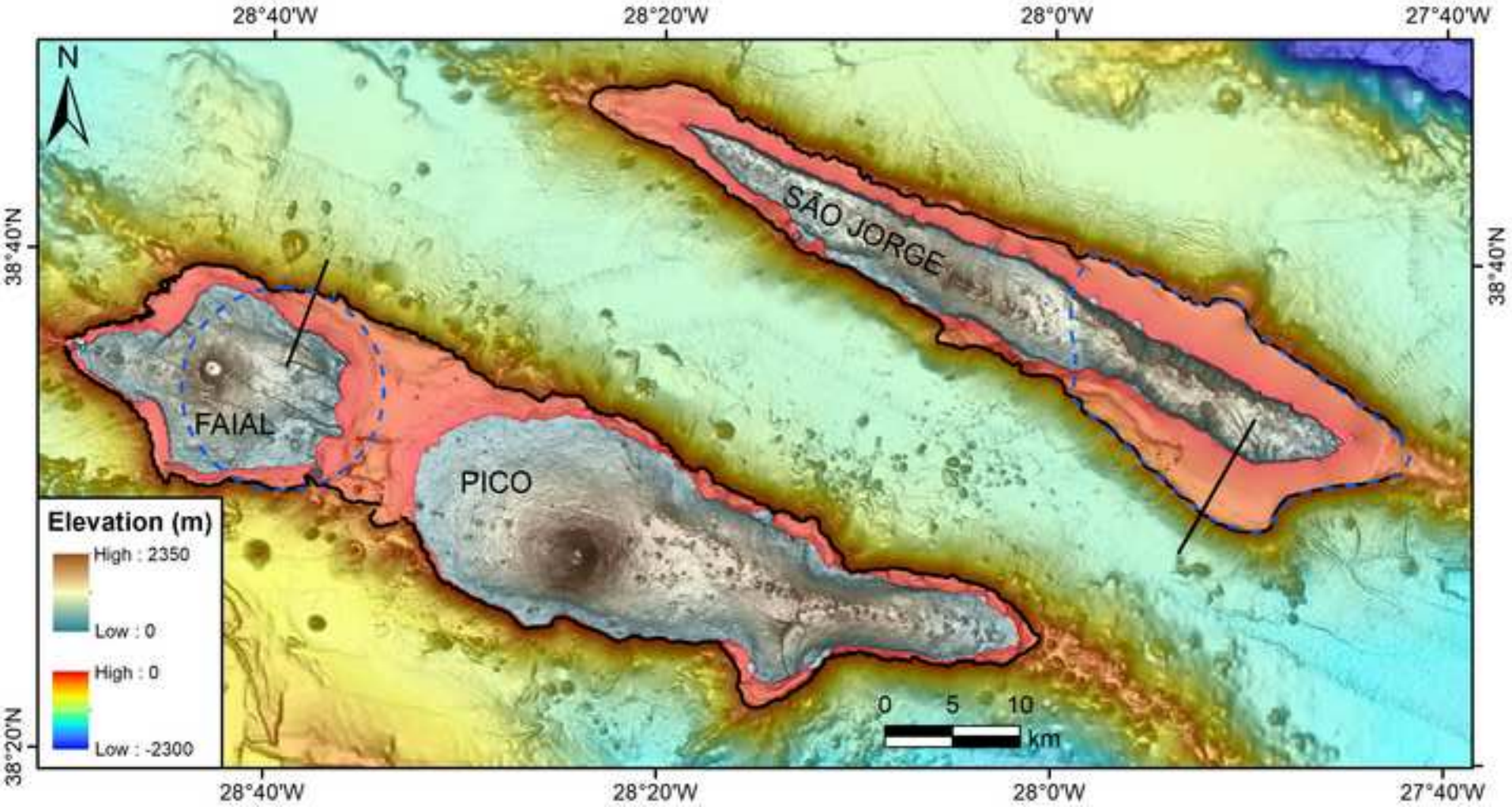

Figure 2

Click here to download high resolution image

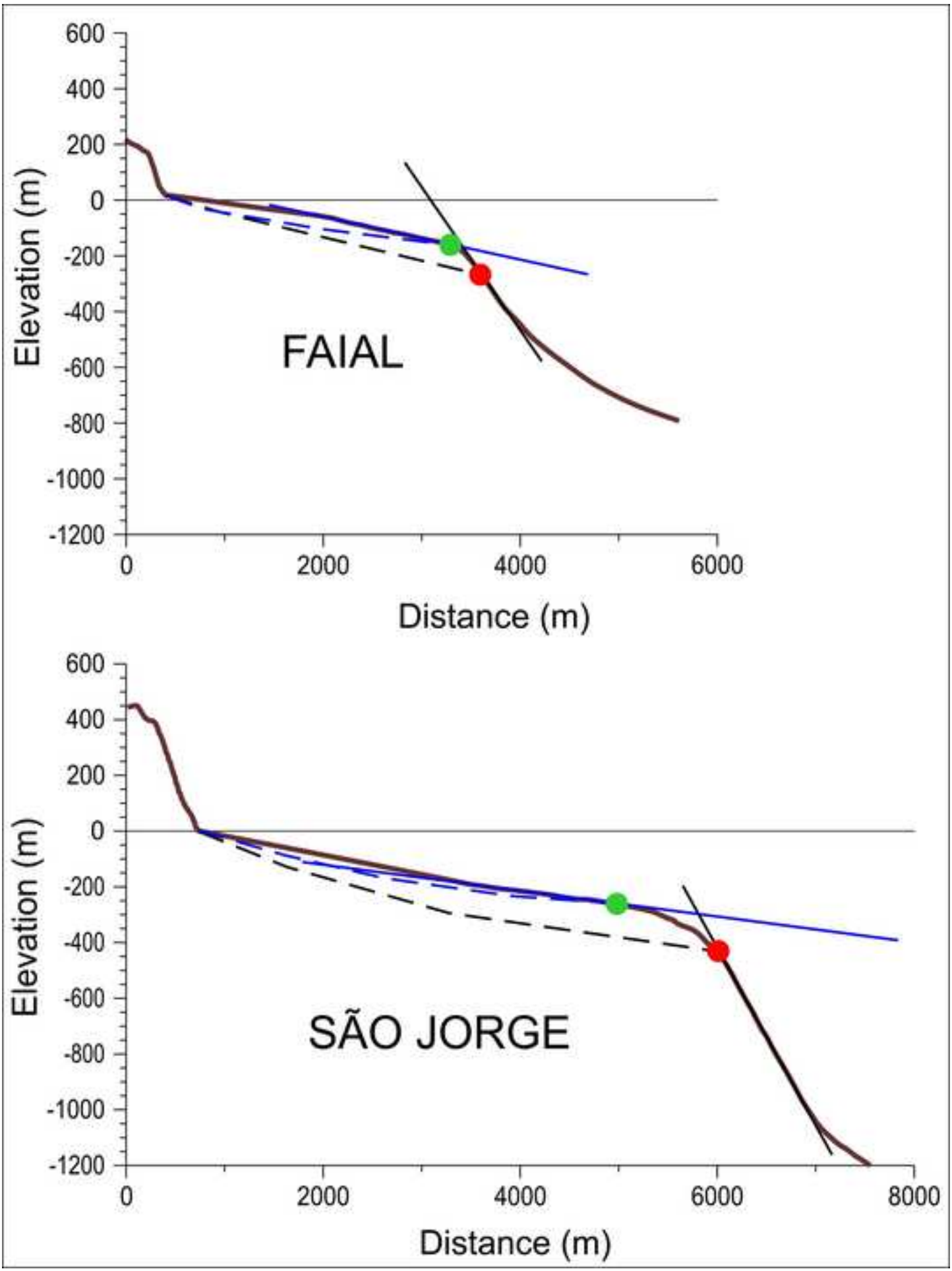

Figure 3

Click here to download high resolution image

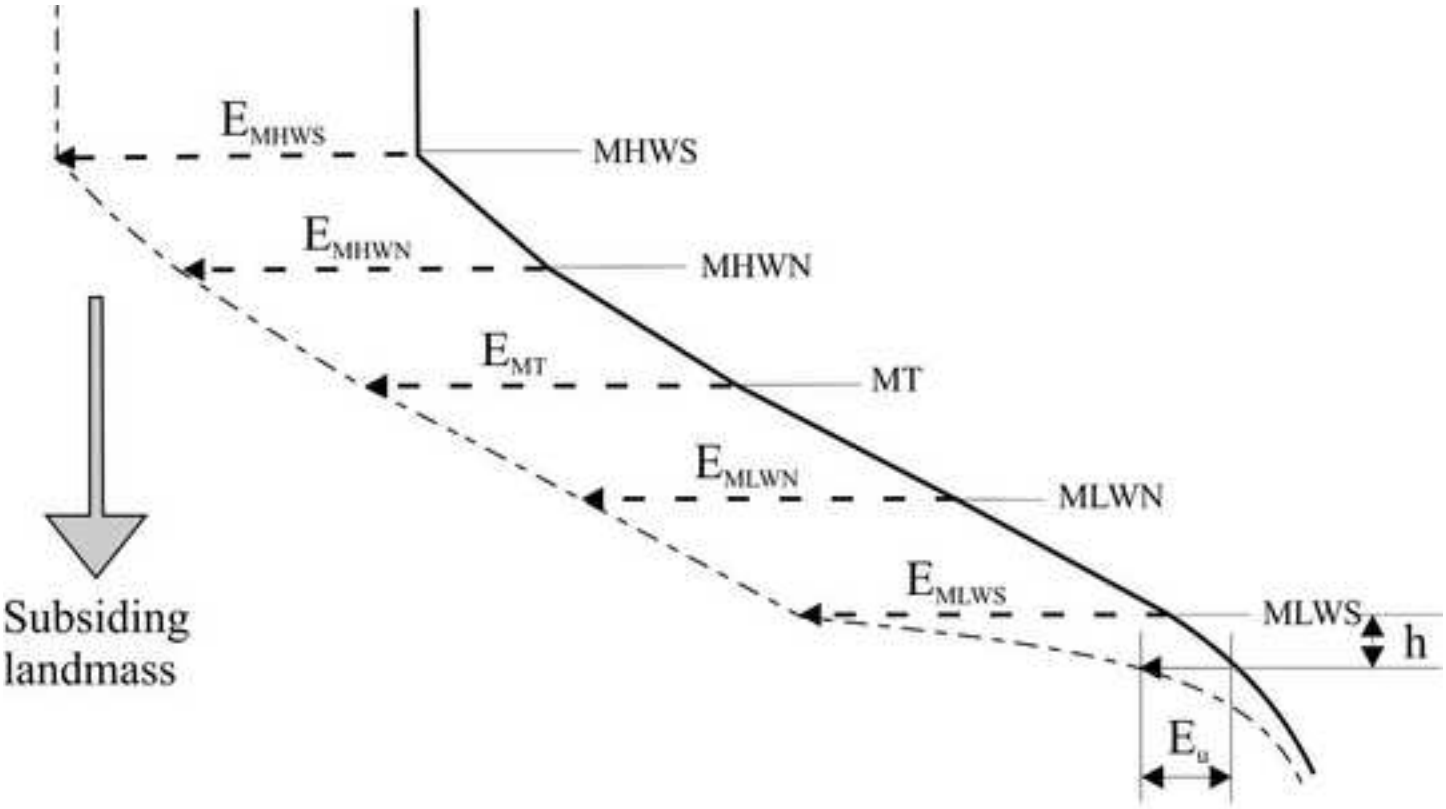

a) in the intertidal zone (Tr = tidal range):

At the MHWS tidal level: $E_{MHWS} = MT_{d(MHWS)} W_n (656\ H_b e^{-kWs} - \tau_c)$

At the MHWN tidal level: $E_{MHWN} = MT_{d(MHWN)} W_n (656\ H_b e^{-kWs} - \tau_c) + E_{MHWS}\ e^{s(Tr/4)}$

At the MT tidal level: $E_{MT} = MT_{d(MT)} W_n (656\ H_b e^{-kWs} - \tau_c) + E_{(MHWS)}\ e^{s(Tr/2)} + E_{(MHWN)}\ e^{s(Tr/4)}$

etc

b) below the intertidal zone (below MLWS)

$$E_u = E_{MLWS}\ e^{sh}$$

Figure 4

Click here to download high resolution image

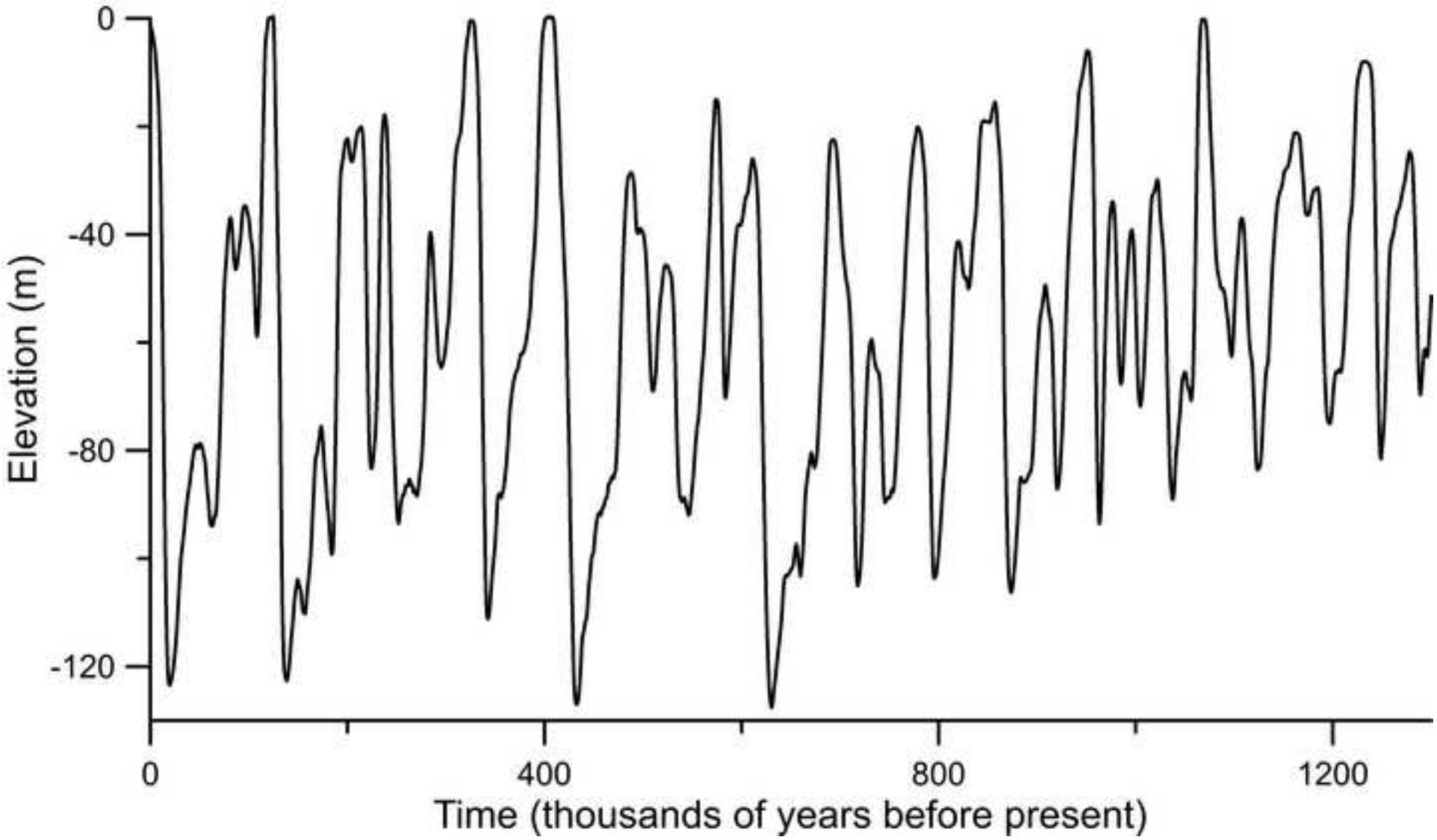

Figure 5

Click here to download high resolution image

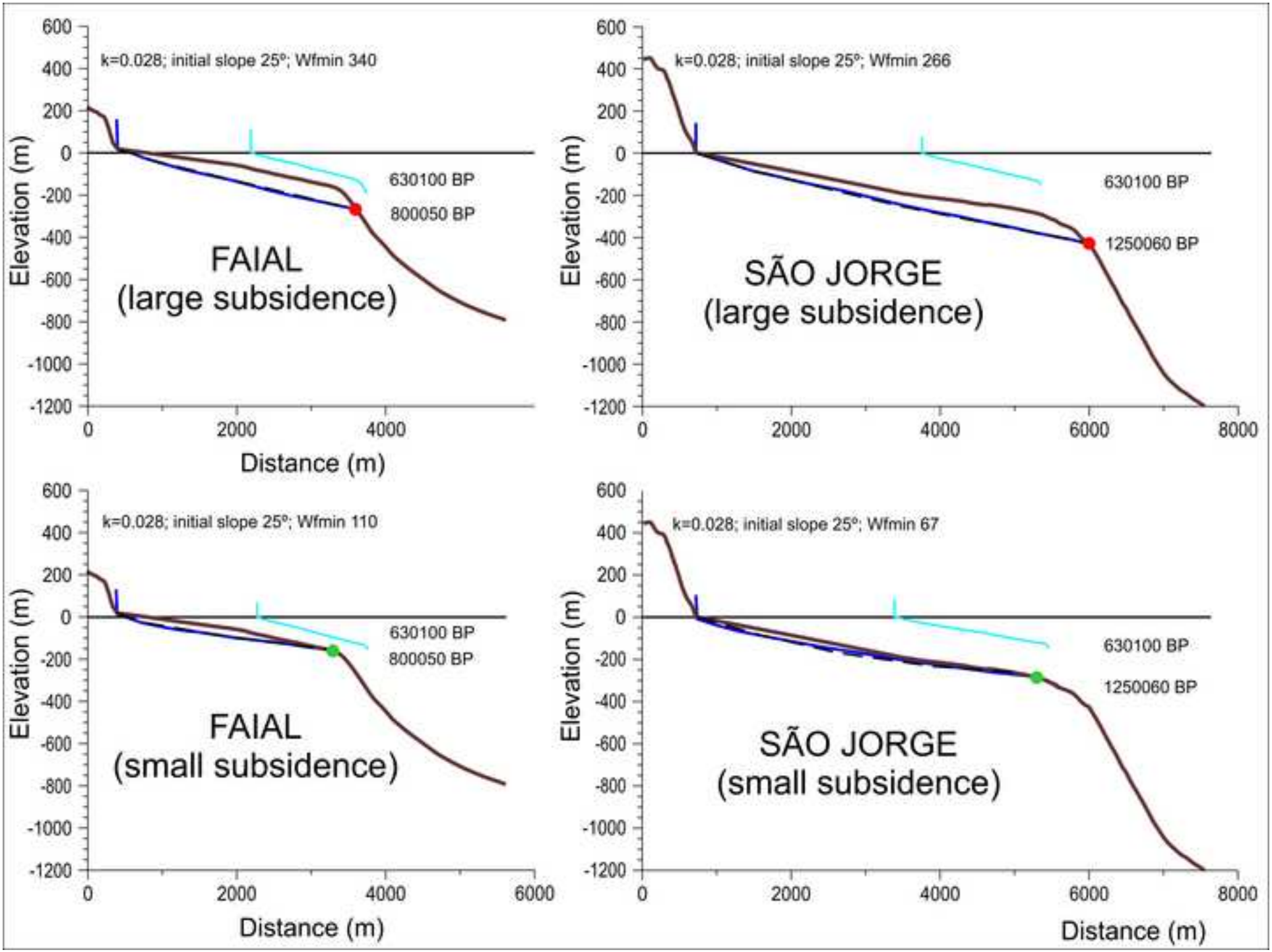

Figure 6

Click here to download high resolution image

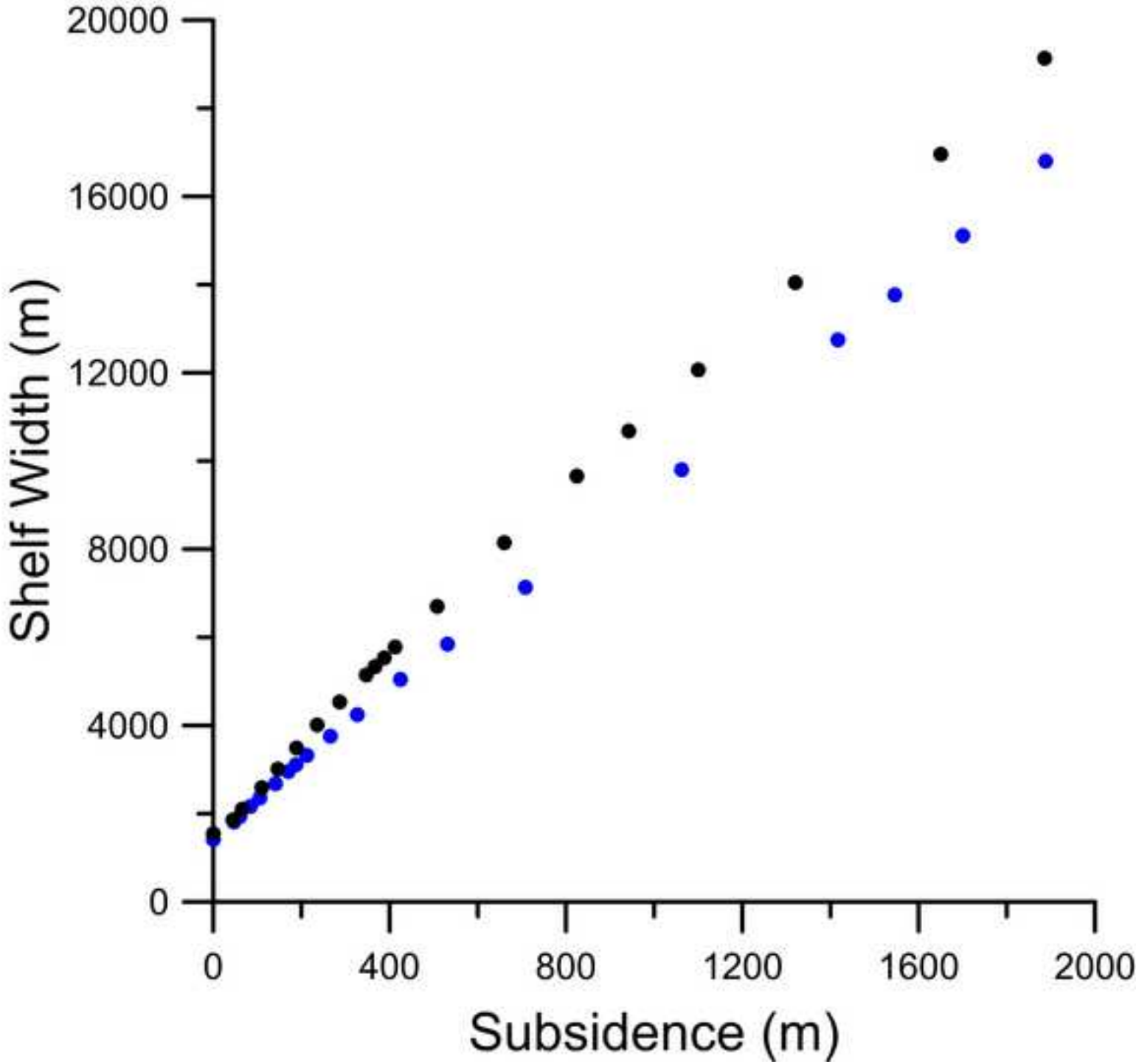

Supplementary material (Figures)

Click here to download Supplementary material for online publication only: Supplementary_material.docx